Frontiers in Bioscience Landmark

Front. Biosci. (Landmark Ed) **2023**; 28(12): 336
https://doi.org/10.31083/j.fbl2812336

Original Research

Genotypic Characterization of a Chinese Family with Osteogenesis Imperfecta and Generation of Disease-Specific Induced Pluripotent Stem Cells

Dandan Li[1,2,3,†], Minglin Ou[1,4,†], Guandong Dai[5,†], Peng Zhu[5], Qi Luo[1], Jieping Chen[1], Zahir Shah[6], Igor M. Samokhvalov[6,7], Lianghong Yin[2], Guoping Sun[5,*], Donge Tang[1,*], Yong Dai[1,8,*]

[1]Clinical Medical Research Center, The Second Clinical Medical College of Jinan University (Shenzhen People's Hospital), 518020 Shenzhen, Guangdong, China
[2]Institute of Nephrology and Blood Purification, The First Affiliated Hospital, Jinan University, 510632 Guangzhou, Guangdong, China
[3]Experimental Center, Shenzhen Pingle Orthopedic Hospital (Shenzhen Pingshan Traditional Chinese Medicine Hospital), 518118 Shenzhen, Guangdong, China
[4]Central Laboratory, Guangxi Health Commission Key Laboratory of Glucose and Lipid Metabolism Disorders, The Second Affiliated Hospital of Guilin Medical University, 541199 Guilin, Guangxi, China
[5]Department of Orthopedics, Department of Radiology, Shenzhen Pingshan District People's Hospital (Pingshan General Hospital, Southern Medical University), 518110 Shenzhen, Guangdong, China
[6]CAS Key Laboratory of Regenerative Biology, Guangdong Provincial Key Laboratory of Stem Cells and Regenerative Medicine, Guangzhou Institutes of Biomedicine and Health, Chinese Academy of Sciences, 510530 Guangzhou, Guangdong, China
[7]Engineering Center for Genetic and Cellular Biotechnology, V. I. Vernadsky Crimean Federal University, 295007 Simferopol, Republic of Crimea
[8]The First Affiliated Hospital, School of Medicine, Anhui University of Science and Technology, 232001 Huainan, Anhui, China
*Correspondence: 15816883398@163.com (Guoping Sun); donge66@126.com (Donge Tang); daiyong22@aliyun.com (Yong Dai)
[†]These authors contributed equally.

Academic Editor: Elisa Belluzzi
Submitted: 19 July 2023 Revised: 19 October 2023 Accepted: 25 October 2023 Published: 12 December 2023

Abstract

Background: Osteogenesis imperfecta (OI) is a rare genetic disorder characterized by recurring bone fractures. Some OI patients have other clinical manifestations such as growth retardation, dental abnormalities, blue sclera, and hearing loss. The relationship between the phenotype and genotype of OI is indistinct, and there is no cure for OI. Therefore, an appropriate disease model is urgently needed to understand the pathophysiology of OI. Induced pluripotent stem cells (iPSCs) are capable of developing into three germ layers and have the same genetic background as the donor cells they were derived from; thus, they are an appropriate disease model. **Methods**: Blood samples collected from the proband and her affected children and one unaffected child were used for genotyping by whole genome sequencing. A patient-specific iPSC line and a healthy donor iPSC line were generated by reprogramming peripheral blood mononuclear cells with episomal plasmids containing seven transcription factors, namely, *OCT4*, *SOX2*, *NANOG*, *LIN28*, *cMYC*, *KLF4*, and *SV40LT*. **Results**: The proband and her two affected children were homozygous for a mutation in collagen type I alpha 1 exon 10, c.725G>T, predicting a p.G242V substitution. A patient-specific iPSC line and a healthy donor iPSC line were generated and characterized in terms of their human embryonic stem cell-like morphology, expression of pluripotency markers, and the ability to differentiate into cells of three germ layers. **Conclusions**: Here, we report the phenotyping and iPSC disease modeling of an OI family. The detailed phenotyping of the OI family and establishment of iPSCs from an OI patient and healthy family member will provide a powerful tool to evaluate the pathophysiology of OI and develop targeted therapies.

Keywords: genotyping; osteogenesis imperfecta; whole genome sequencing; collagen type I alpha 1; induced pluripotent stem cells

1. Introduction

Osteogenesis imperfecta (OI) is a rare and intractable heterogeneous hereditary condition characterized by bone fragility and systemic complications including bone deformity, delayed growth, dental abnormalities, blue sclera, hearing loss, cardiovascular disorders, and ligament relaxation [1,2]. Its clinical features are heterogeneous, ranging in severity from benign to perinatal fatal [3,4]. Despite sharing the same causative mutant genes, the clinical manifestations usually significantly differ among patients [5]. Although approximately 20 OI causative genes have been reported [6], the majority of OI cases are caused by pathogenic variants in the genes encoding collagen type I alpha-1 (COL1A1) and collagen type I alpha-2 (COL1A2), resulting in synthesis defects of type I collagen [7–9], which is the primary structural protein of bone [10]. Despite the significant progress that has been made in identifying the pathogenic genes and understanding the molecular causes of OI, the exact pathogenesis of OI remains unclear [11].

Furthermore, there is limited knowledge on the relationship between the OI phenotype and its genotype [1], and no cure is available for OI [12]. Osteoblasts from OI patients, which display OI-relevant features, are reasonable study models for OI investigation; however, obtaining osteoblast samples from OI patients is challenging. Thus, it is important to develop disease models that can, to some extent, better replicate disease-related characteristics. This will aid in understanding the pathophysiology of OI and assessing potential drug treatments.

Induced pluripotent stem cells (iPSCs) are an ideal source for developing such models [13–15], as they retain the genetic information from the donor cells and have the capacity for unlimited propagation as well as the potential to differentiate into three different cell lineages [16]. It is worth noting that iPSCs are not subject to immune rejection or ethical concerns [17] and can be constructed from a wide range of source cells [18]. Due to these advantages, many disease-specific iPSCs have been successfully established, and have become an indispensable research tool for medical, pharmaceutical, and biological research.

Here, we report the study of an OI family. The proband and her two affected children had a heterozygous mutation, c.725G>T (p.G242V) in exon 10 of *COL1A1*. The family was diagnosed OI type I (OMIM #166200). We generated a peripheral blood monocyte (PBMC)-derived OI patient-specific iPSC line (OI-iPSC) and a healthy donor iPSC line (HC-iPSC). These iPSC lines were characterized based on their morphology resembling human embryonic stem cells (hESCs), the expression of markers associated with pluripotency, and their ability to undergo differentiation into cell types representative of the three primary germ layers. The successful genotyping of the OI family and establishment of iPSCs from an OI patient and a healthy family member will provide a powerful tool to evaluate the pathophysiology of OI and develop targeted therapies.

2. Methods

2.1 Human Samples

This study received approval from the Medical Ethics Committee of Shenzhen People's Hospital (Shenzhen, China), in accordance with the ethical guidelines outlined in the Declaration Helsinki for conducting medical research involving human subjects. All subjects included in this study gave written informed consent to participate. The permission was obtained from the participants to use their photographs. Animal studies were approved by Jinan University Laboratory Animal Ethics Committee (20210301-38). Blood samples were collected from participant donors within a family affected by OI after their informed consent (Fig. 1H), including the proband (I-1), her two affected children (II-4 and II-5) and her one unaffected child (II-1), and 100 unrelated, healthy and ancestry-matched subjects (50 males and 50 females). Human PBMCs were separated from blood samples trough density gradient centrifugation using the Ficoll gradient (Cat. No. 17-1440-03; GE Healthcare, Little Chalfont, Buckinghamshire, UK). The PBMCs were mycoplasma-free, as confirmed by a polymerase chain reaction (PCR) method. Genomic DNA was extracted with a HiPure Blood DNA Mini Kit according to the manufacturer's instructions (Magen, Guangzhou, China). The detailed procedure is provided in the supporting information.

2.2 Genotyping by Whole Genome Sequencing

Whole genome sequencing (WGS) of I-1, II-1, II-4 and II-5 was performed using the Hiseq X Ten system (Illumina, San Diego, CA, USA). The clean data were obtained after filtering and alignment to the reference human genome (GRCh37/HG19). After deduplication, barcode correction, local realignment, and base quality recalibration, the processed data were subjected to detection of single nucleotide polymorphisms (SNPs) and insertions/deletions (Indels). The obtained variant detection results were compared with entries in databases. The candidate variants were screened using a list of OI genes (**Supplementary Table 1**). The detailed procedure is provided in the supporting information.

2.3 COL1A1 Mutation Confirmation

PCR amplification was conducted with the GeneAmp PCR System 9700 Thermal Cycler (Applied Biosystems, Waltham, MA, USA). After purification by agarose gel electrophoresis, the PCR products were subjected to analysis using the ABI 3730 DNA Genetic Analyzer (Applied Biosystems, Foster City, CA, USA). The results were compared to the *COL1A1* gene sequence using Chromas software 2.6.6 (Technelysium, South Brisbane, QLD, Australia, http://technelysium.com.au/wp/chromas/). The detailed procedure is provided in the supporting information.

2.4 PBMC Cell Culture and Generation of iPSCs

PBMCs were seeded in a 6-well plate coated with fibronectin and cultured in PBMC medium for 7 days. Then PBMCs were collected and suspended in an electroporation reaction solution, along with a plasmid mixture (pEP4EO2SEN2K, pEP4EO2SET2K, pCEP4-M2L, **Supplementary Fig. 1**). After electroporation using the Amaxa Nucleofector II Transfection Device (Amaxa, Cologne, Germany), the PBMCs were cultured overnight in StemSpan Serum Free Expansion Medium supplemented with cytokines in a 6-well plate coated with fibronectin and Matrigel. The next day, the culture medium was replaced with Dulbecco's Modified Eagle Medium/F12 and supplemented with N-2, B-27, and other specified components. The medium was replaced daily. After 11 days, the culture medium was switched to NuwaCell hPSC Medium. Manually selected ESC-like colonies were cultured in a 6-well plate coated with Matrigel for expansion. The detailed procedure is provided in the supporting information.

2.5 Short Tandem Repeat Profiling

To verify the source of the constructed iPSC lines, genomic DNAs from both iPSC lines and their parental cells were employed for short tandem repeat (STR) profiling. In brief, genomic DNAs were extracted using the Chelex 100 resin and amplified. The PCR products were electrophoresed and analyzed using the ABI 3500XL Genetic Analyzer (Applied Biosystems, Foster City, CA, USA). The genetic profiles were analyzed utilizing the PowerPlex® 21 PCR Amplification System (Promega, Madison, WI, USA) targeting the 21 loci markers. For a detailed description of the procedure, please refer to the supporting information.

2.6 mRNA Isolation and Quantitative Polymerase Chain Reaction

Total RNA was extracted employing the RNAprep Pure Cell/Bacteria Kit (TIANGEN, China). Then PCR reactions were conducted with the LightCycler 96 Real Time PCR System (Roche, Basel, Switzerland), and the data were assessed utilizing LightCycler software (version 1.1.0.1320, Roche, Basel, Switzerland). The primers listed in **Supplementary Table 2** were used to assess the expression of octamer-binding transcription factor 4 (*OCT4*, also known as *POU5F1*) and Nanog homeobox (*NANOG*). The detailed procedure is provided in the supporting information.

2.7 Flow Cytometry

The anti-bodies listed in **Supplementary Table 3** were used for the immunostaining of cells, and the Gallios Flow Cytometer (Beckman Coulter, Brea, CA, USA) was utilized to assess the cells.

2.8 Determination of Karyotype

G-banding karyotype analysis was conducted to determine the karyotype of the iPSC lines. The iPSCs were collected when they reached about 60% confluence, and chromosome G-banding analysis specimens were prepared using a standard method. A total of 20–30 metaphases were analyzed. The detailed procedure is provided in the supporting information.

2.9 Pluripotency Validation in Vivo

The teratoma assay was conducted to analyze the pluripotency of iPSCs *in vivo*. After resuspending in a mixture of 50% Matrigel and phosphate-buffered saline (PBS), iPSCs were injected into the posterior thigh muscles of 4-week-old SCID Beige mice. At 8 weeks post-injection, the mice were euthanized and the tumors were collected and subjected to hematoxylin and eosin (H&E) staining. The detailed procedure is provided in the supporting information.

2.10 Detection of Mycoplasma and Pathogenic Microorganism

Mycoplasma contamination was verified through PCR analysis. The absence of pathogenic microorganism contamination (hepatitis B virus (HBV), hepatitis C virus (HCV), human immunodeficiency virus (HIV), syphilis) was verified by an accredited clinical laboratory service provider (Hefei KingMed for Clinical Laboratory, Anhui, China).

2.11 Detection of Exogenous Genes

The detection of exogenous genes was performed using the quantitative PCR (qPCR) standard curve method. Briefly, 0, 0.1, 1, 10, and 100 copies of plasmids were mixed with pure mesenchymal stem cells (MSCs). After DNA was extracted from each group, qPCR was performed with the LightCycler480 System (Roche, Alameda, CA, USA). The primers are listed in **Supplementary Table 4**. *OCT4* was used as the endogenous control gene, and the $2^{-\Delta\Delta Ct}$ method was applied to assess the expression of Epstein-Barr nuclear antigen 1 (*EBNA1*) in the iPSCs.

3. Results

3.1 Clinical Features of OI Patients

The proband (I-1), a 53-year-old Chinese woman, received a diagnosis of OI type I. At the age of 10, she had a fracture of the left elbow but took no medication, which resulted in left cubitus varus. Subsequently, bone fractures occurred more than 20 times, particularly in her hands, waist, legs and feet. Physical examination at 53 years old showed a short stature, height of 120.1 cm and weight of 50.9 kg, blue sclera, dentinogenesis imperfecta, normal hearing and vision, left cubitus varus, bending deformities of thighs, and osteoporosis (Table 1, Fig. 1C and **Supplementary Fig. 2**). Full-body radiographs revealed low bone mineral density in the long tubular bones, widening of the long tubular bones, slight curvature of the backbone, and multiple pathological fractures with malunion (Fig. 1A,B and **Supplementary Fig. 3**). The proband was married to a healthy man. She had been pregnant 10 times, with three spontaneous abortions (Fig. 1H). She had seven children (4 boys and 3 girls), of whom one boy and one girl had OI (Fig. 1H).

The proband's affected son (II-4), a 27-year-old male, was diagnosed with OI type I. His first brittle fracture occurred at 15 years old. He had experienced more than 10 bone fractures, particularly in his hands, waist, and legs. He exhibited blue sclerae and scoliosis with hearing loss, but no dentinogenesis imperfecta (Table 1). At 27 years old his weight was 59.8 kg and his height was 149.8 cm. X-ray films indicated a small skull base and thin facial bone, enlarged cranial bone, slight curvatures of the long tubular bones, and widening of the radius (Fig. 1D,E and **Supplementary Fig. 4**).

Table 1. Clinical features of the three patients with OI type I.

Characteristics	Patients		
	I-1	II-4	II-5
Clinical findings			
Sex	Female	Male	Female
Age, years	53	27	24
Weight, kg	50.9	59.8	45.0
Height, cm	120.1	149.8	139
Disease severity	Severe	Moderate	Moderate
Skeletal findings			
Multiple fractures of extremities	Yes	No	No
Age at first fracture, years	10	15	6
Vertebral fractures	No	No	No
Bowing of upper extremities	Yes	No	No
Bowing of lower extremities	Yes	No	No
Shortening of upper extremities	Yes	No	No
Shortening of lower extremities	Yes	No	No
Spine abnormalities	Yes	No	No
Scoliosis	Yes	Yes	Yes
Other findings			
Color of sclera	Blue	Blue	Blue
Dentinogenesis imperfecta	Yes	No	No
Hypermobility of joints	Yes	No	No
Cardiac impairment	No	No	No
Hearing impairment	No	Yes	No
Intellectual development	Normal	Normal	Normal
Therapy			
Bisphosphate treatment	Yes	No	No
Right patella fixation	Yes	No	No

OI, osteogenesis imperfect.

The affected daughter (II-5) is 24 years old and was also diagnosed with OI type I. Her first brittle fracture occurred at 6 years old. She exhibited blue sclera and scoliosis, with no dentinogenesis imperfecta (Table 1). Her vision and hearing were normal. At 24 years old, her weight was 45.0 kg and her height was 139 cm. The X-ray revealed a small skull base and thin facial bone, enlarged cranial bone, slight curvatures of the long tubular bones and widening of the radius (Fig. 1F,G and **Supplementary Fig. 5**).

3.2 Genotyping of the OI Family

Of the total 470 Gbp sequencing data, more than 100 Gbp high-quality sequencing data with an average of 99.0% coverage were obtained (**Supplementary Table 5**). The valid sequencing depth ranged from 31.6× to 35.3× (**Supplementary Table 6**). The rate of SNP/InDel detection was between 3 and 5 million, according to routine detection (**Supplementary Tables 5,6**). Quality control of the identified DNA variants was performed by comparing with entries in the National Center for Biotechnology Information Single Nucleotide Polymorphism (NCBI dbSNP), 1000 Genomes Project, and Exome Sequencing Project v.6500 (ESP6500) databases. A total of 227 rare mutations for altering the protein-encoding amino acids were identified in the sample from I-1, 216 from II-1, 214 from II-4 and 186 from II-5. Considering that OI is a hereditary disease, 25 candidate rare mutations in different genes including *SPEN*, *EIF4G3*, *MACF1*, *DPYD*, *CDON*, *ZBTB44*, *IGSF9B*, *RIMBP2*, *PDX1*, *KRT14*, *COL1A1*, *LRRC37A3*, *MRPL12*, *PSG6*, *LILRA2*, *USP29*, *SFT2D3*, *HIC2*, *XRN1*, *WDR36*, *SGCD*, *HLA-DRB1*, *TTBK1*, *TJAP1* and *SAPCD2* among the affected family members were identified (**Supplementary Table 7**). We directed our attention to the OI genes documented in the database (**Supplementary Table 1**) and identified a plausible causative variant within *COL1A1* (chr17: g.48274566 C>A [NM_000088.3, c.725G>T, p.G242V]).

As shown in Fig. 1I, PCR and Sanger sequencing revealed that the proband and her two affected children carried the heterozygous G242V mutation, whereas the healthy family member and the 100 population-matched controls did not exhibit the mutation. One patient with OI has been reported to harbor the heterozygous c.725G>A (p.G242V) mutation in *COL1A1* [19] (https://databases.lovd.nl/shared/diseases/05296). Cross-species amino acid comparison of *COL1A1* demonstrated that this site was highly conserved (Fig. 1J).

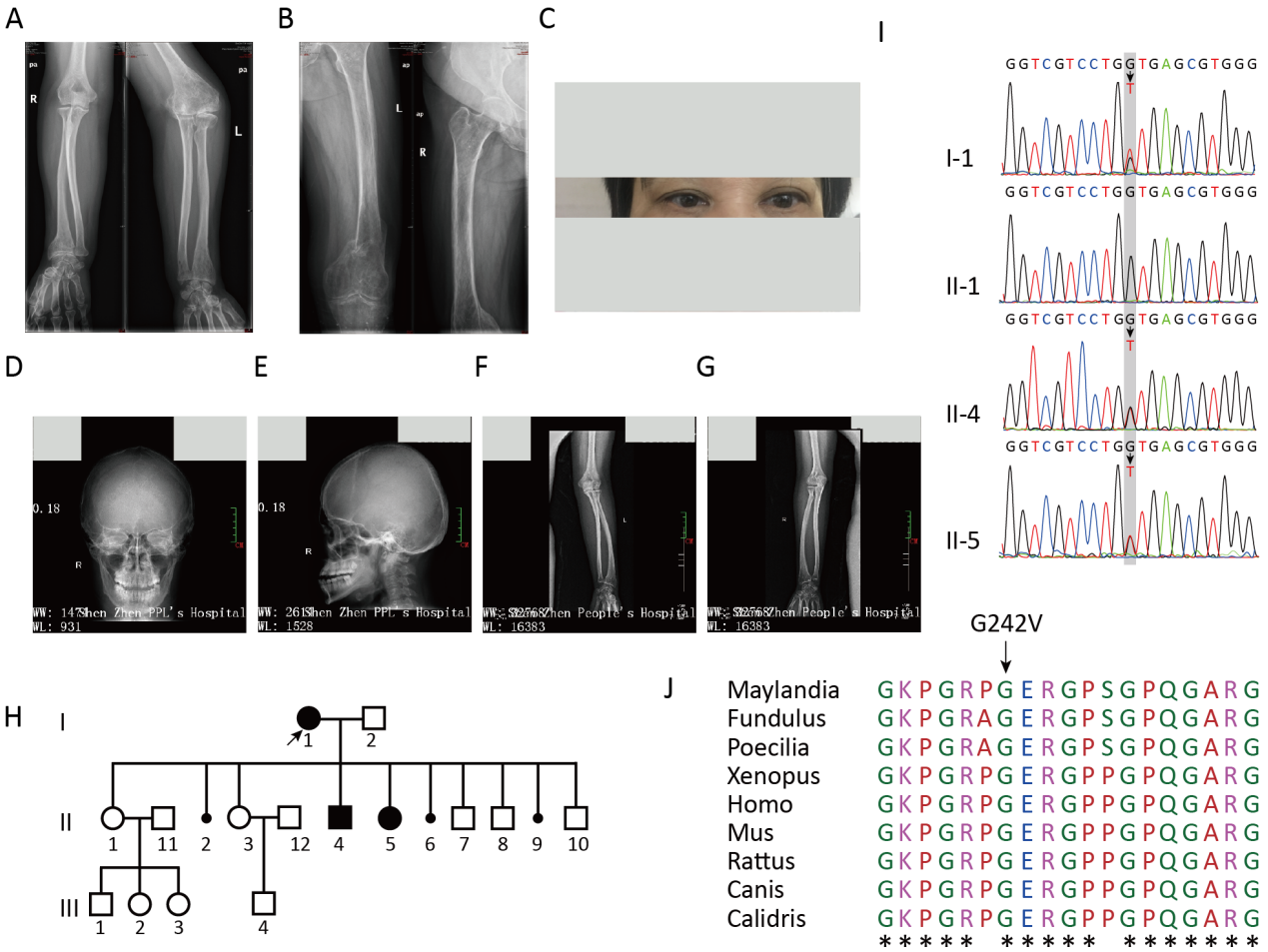

Fig. 1. Clinical and radiographic features of OI patients and genotyping of the OI family. (A,B) Radiographs of the proband. (C) Photographs of the proband showed blue sclera. (D,E) Radiographs of the proband's affected son. (F,G) Radiographs of the proband's affected daughter. (H) Pedigree of the OI family recruited to this study. (I) A point mutation, c.725G>T, was heterozygous in the three OI patients, as determined by PCR and DNA sequencing. (J) Alignment of the amino acid sequence of COL1A1 among several species. PCR, polymerase chain reaction; COL1A1, collagen type I alpha-1.

3.3 Generation and General Characteristics of OI-iPSCs and HC-iPSCs

To generate iPSCs, PBMCs taken from II-1 and II-4 were expanded and transfected with episomal vectors expressing pluripotency factors (*OCT4*, *SOX2*, *NANOG*, *LIN28*, *cMYC*, *KLF4* and *SV40LT*) under feeder-free conditions [20]. Typical iPSC colonies with a morphology resembling hESCs were manually selected and expanded on Matrigel-coated plates with passages conducted every 3–4 days.

As depicted in Fig. 2A,B, OI-iPSCs showed typically hESC-like morphological features. Flow cytometry analyses revealed that OI-iPSCs were positive for the pluripotency surface markers stage-specific embryonic antigen-4 (SSEA-4) and TRA-1-81 (Fig. 2C,D). The expression of pluripotent stem cell markers (*OCT4*, *NANOG*) was also confirmed by qPCR analysis (Fig. 2E). For qPCR analysis, the MSC line P3 (MSC-P3) served as a negative control, whereas the hESC line H1 (hESC-H1) served as a positive control. Chromosome GTG band analysis showed that OI-iPSCs exhibited a normal diploid 46, XY karyotype (Fig. 2F). To assess the *in vivo* pluripotency of OI-iPSCs, the teratoma formation assay was conducted. OI-iPSCs were injected into SCID Beige mice, and the teratomas were harvested 8 weeks after injection. H&E staining confirmed the presence of derivatives from all three germ layers in the teratomas, such as the neural rosettes formed from the ectoderm, the cartilage differentiated from the mesoderm, and the intestinal epithelial cells developed from the endoderm (Fig. 2G–I). These results provide evidence for the establishment of OI-iPSCs and their pluripotency and ability to undergo multilineage differentiation.

hESC-like morphology was also observed for HC-iPSCs (Fig. 3A,B). The expression of SSEA-4 and TRA-1-81 in HC-iPSCs was evaluated by flow cytometry analysis (Fig. 3C,D). The qPCR assay demonstrated that the endogenous pluripotency genes *OCT4* and *NANOG* were

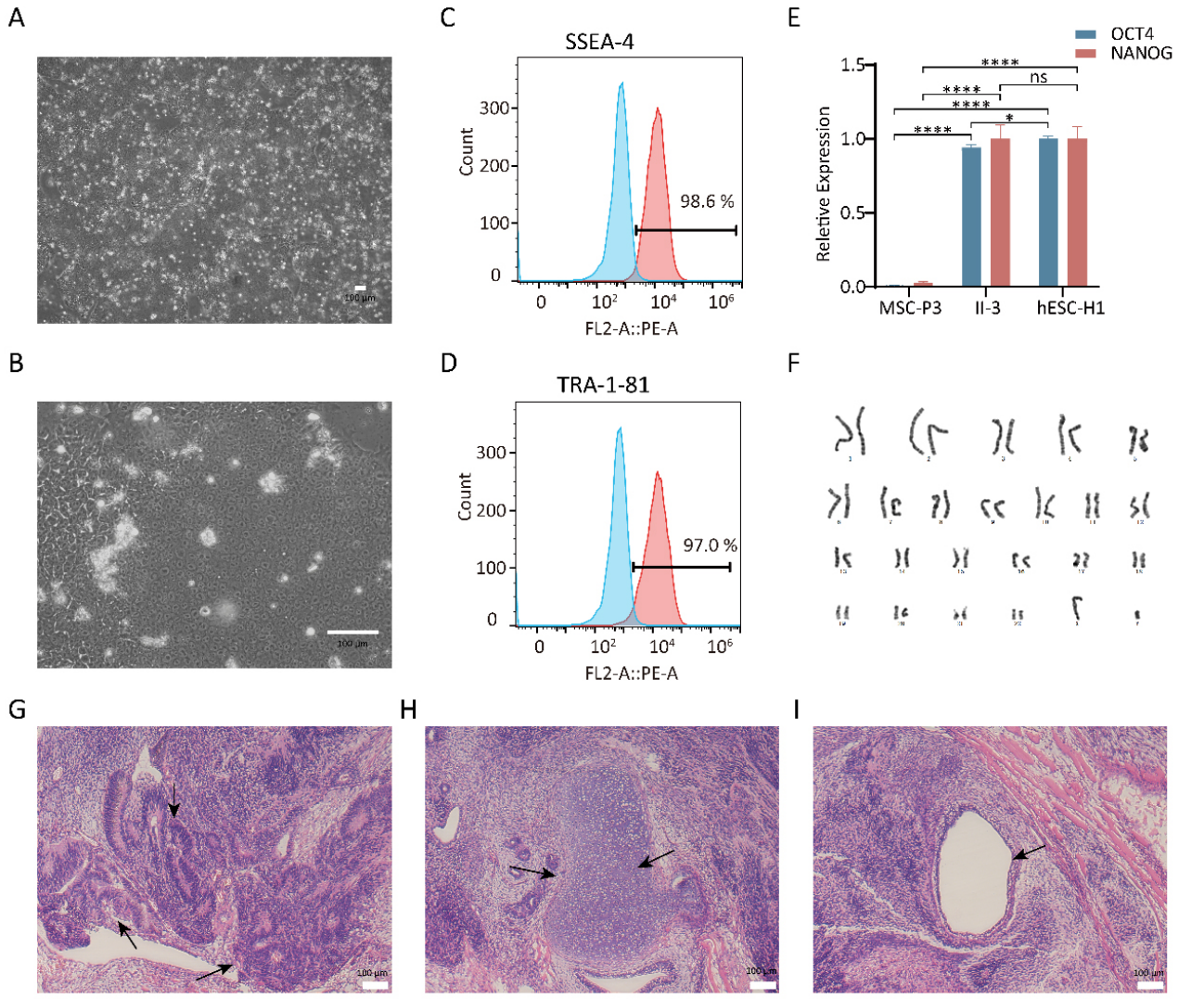

Fig. 2. Characterization of OI-iPSCs. (A,B) Images of OI-iPSC colonies cultured on Matrigel. Scale bar: 100 µm. (C,D) Flow cytometry analysis of pluripotency markers SSEA-4 and Tra-1-81 of OI-iPSCs. (E) Quantification via qPCR analyses of the relative expression levels of the pluripotency markers *OCT4* and *NANOG* in OI-iPSCs (n = 3). (F) OI-iPSCs displayed a normal karyotype. (G–I) H&E staining of teratomas derived from immunodeficient mice injected with OI-iPSCs showed tissues representing all three embryonic germ layers: ectoderm (neural rosettes), mesoderm (cartilage) and endoderm (intestinal epithelial cells). Scale bar: 100 µm. SSEA-4, stage-specific embryonic antigen-4; OI-iPSC, OI patient-specific iPSC line; iPSC, induced pluripotent stem cells; H&E, hematoxylin and eosin (* $p < 0.05$, **** $p < 0.001$, ns nonsignificant).

activated in HC-iPSCs and hESC-H1 cells, whereas they were silenced in MSC-P3 cells (Fig. 3E). HC-iPSCs exhibited the normal karyotype of diploid 46 XX by standard G-banding chromosome analysis (Fig. 3F). The teratoma assay detailed previously was conducted to assess the pluripotency of HC-iPSCs. H&E staining verified the nature of these tumors as teratomas, as evidenced by the presence of tissues representing all three germ layers including neural epithelia (Fig. 3G), cartilage (Fig. 3H) and intestinal epithelia (Fig. 3I). These results indicated the successful generation and functional pluripotency of HC-iPSCs.

3.4 STR Loci Analysis and Mycoplasma and Pathogenic Microorganism Detection for OI-iPSCs and HC-iPSCs

STR analysis demonstrated that OI-iPSCs and HC-iPSCs displayed the same 21 STR loci as their parental PBMC cells (**Supplementary Tables 8,9**). Mycoplasma detection confirmed the absence of mycoplasma contamination in both iPSC lines (**Supplementary Fig. 6**). The absence of pathogenic microorganism contamination was also confirmed for OI-iPSCs and HC-iPSCs (**Supplementary Tables 10,11**). The negative expression of exogenous genes in both iPSC lines was confirmed using the qPCR standard curve method (**Supplementary Figs. 7,8**).

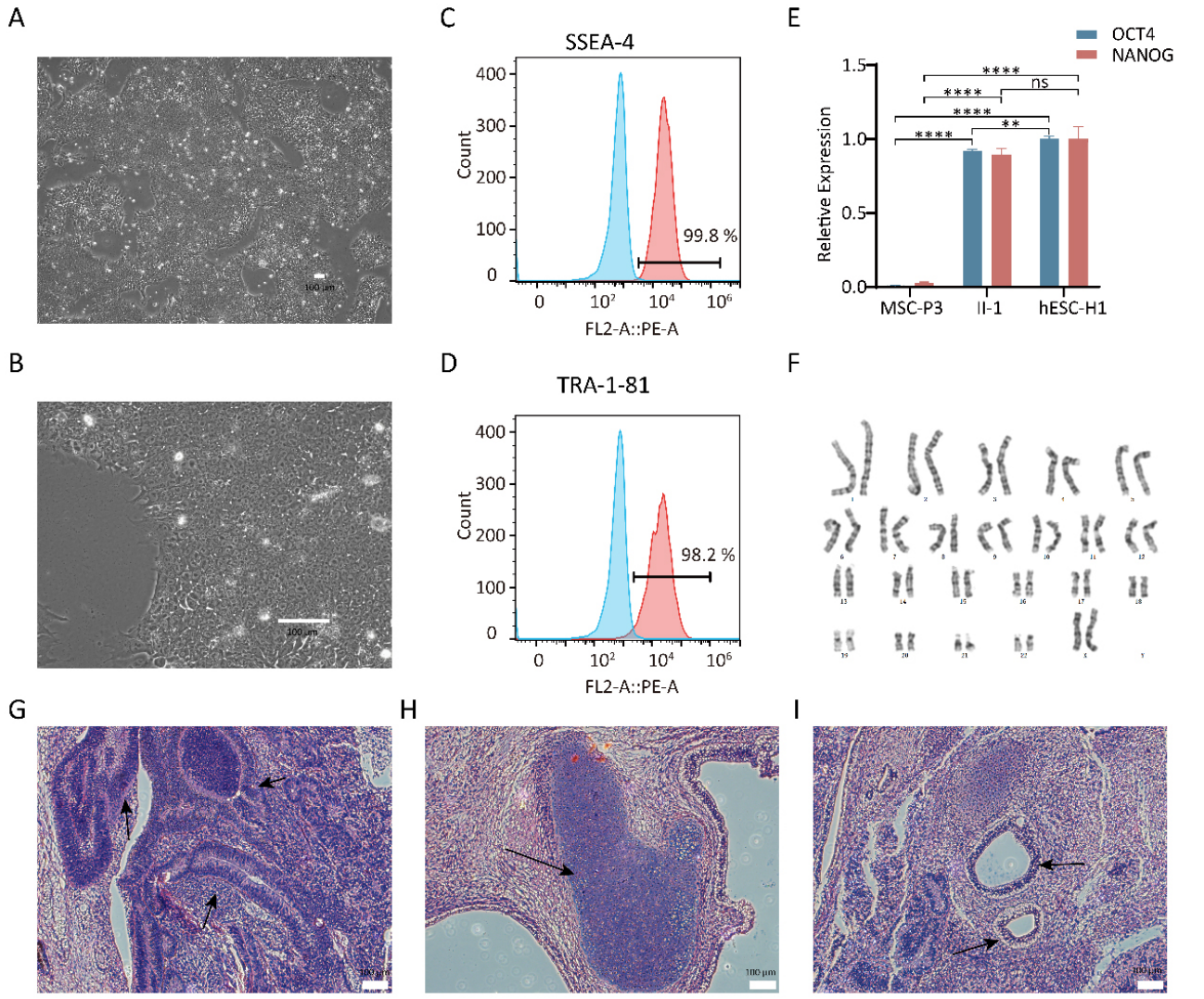

Fig. 3. Characterization of HC-iPSCs. (A,B) Images of HC-iPSC colonies cultured on Matrigel. Scale bar: 100 µm. (C,D) Flow cytometry analysis of pluripotency markers SSEA-4 and Tra-181 of HC-iPSCs. (E) Quantification via qPCR analyses of the relative expression levels of the pluripotency markers *OCT4* and *NANOG* in HC-iPSCs (n = 3). (F) HC-iPSCs displayed a normal karyotype. (G–I) H&E staining of teratomas derived from immunodeficient mice injected with HC-iPSCs showed tissues representing all three embryonic germ layers: ectoderm (neural rosettes), mesoderm (cartilage) and endoderm (intestinal epithelial cells). Scale bar: 100 µm. HC-iPSC, healthy donor iPSC line. (** $p < 0.01$, **** $p < 0.001$, ns nonsignificant).

4. Discussion

In 1979, Sillence *et al.* [21] classified OI into four types (type 1 to type IV) based on clinical manifestations, radiological features, and genetic patterns; this classification is referred to as the "Sillence classification". Type 1 OI follows an autosomal dominant inheritance pattern and is characterized by the presence of blue sclerae and mild bone deformities. Type II OI is used to describe the lethal perinatal cases, often indicative of autosomal recessive inheritance. Type III OI is associated with a progressively deforming phenotype, where the blue sclerae tend to fade with age and autosomal recessive inheritance is often observed. Type IV OI is characterized by white sclerae, short stature, bone deformities, and dentin hypoplasia. In this study, we examined a Chinese family displaying clinical characteristics of type I OI inherited in an autosomal dominant fashion. Even carrying the same mutated gene, the three patients exhibited different clinical features. The proband had serious OI symptoms including multiple bone fractures, osteopenia, healing of long bones, scoliosis, dentinogenesis imperfecta, and blue sclera. The affected proband's son had a mild form of OI, such as frequent bone fractures, blue sclera and hearing loss. The affected proband's daughter exhibited a milder form of OI. WGS and Sanger sequencing confirmed a heterozygous mutation in *COL1A1* exon 10, c.725G>T (nucleotide: NM_000088.3, GRCh37) predicting a p.G242V substitution (protein: NP_000079.1). This is a novel mutation in

COL1A1. A different mutation (c.725G>A, p.G242V) was reported at the same nucleotide sites in a male Korean patient with sporadic OI [19]. This is a pathogenic mutation, which supports our results showing that the detected mutation in *COL1A1* (c.725G>T, p.G242V) is the pathogenic mutation for this OI family.

The genes *COL1A1*, situated on chromosome 17q21.3-22, and *COL1A2*, situated on chromosome 7q21.3-q22.1, encode type I collagen [22], the primary component of bone extracellular matrix, which is essential for the mechanical properties of bone [23]. Similar to other collagens, the distinctive structural characteristic of type I collagen is a rod-like trimer structure with a long continuous triple helix motif, which is composed of Gly-X-Y amino acid units [24]. Due to its smallest size, the glycine residues are positioned at the core of the triple helix domain [25]. After produced, the collagen molecules are precisely aligned to form fibers, followed by the parallel growth of hydroxyapatite crystals alongside these collagen fibrils [26]. Once glycine is replaced by a larger amino acid, such as valine, the residue no longer fits within the confined space at the core the triple helix domain, resulting in disturbed helical collagen structure [26]. The abnormal collagen I molecules can impact the mechanical characteristics of bone in two ways [1]. The abnormal collagen matrix leads to reduced bone toughness and the collagen matrix interacts with the mineral phase of bone. The damaged matrix had a dramatic effect on the integration of the mineral content, a critical factor in influencing bone strength. Type I collagen is also extensively distributed throughout other connective tissues, excluding hyaline cartilage such as bone, skin, tendon, ligament, sclera, cornea, and blood vessels [24]. This could to some extent explain clinical heterogeneity of OI patients in our reported family. However, the mechanism by which mutations in *COL1A1* result in the clinical phenotypes of OI remains a subject of debate. The glycine residue in the Gly-Xaa-Yaa repeat is essential to form a triple helix structure. The alteration p.G242V identified in the OI family is located in the triple helix domain of type I collagen. Recent discoveries suggest that aberrant folding and aggregation of type I collagen could be the main reason for collagenopathy in OI [27–29], which provide us with a research direction to study the pathogenic mechanisms of OI associated with *COL1A1* mutations. To delve into this, a suitable biological model is urgently needed.

iPSCs are generated from somatic cells with reprogramming factors [30] and possess the following strong points. First, they have unlimited proliferation capability and the potential to differentiate into cells of three embryonic germ layers of iPSCs [31]. Second, iPSCs are not targets of immunological rejection or ethical concerns [32]. Third, various somatic cells can be used for generating iPSCs such as fibroblasts, keratinocytes, adipose stem cells, cord blood, peripheral blood, neural cells, and urinary cells [18]. Thus, human iPSCs are a powerful tool to model human diseases, especially single gene diseases [33]. Several OI-specific iPSC lines have been reported. An OI-iPSC line carrying a heterozygous *COL1A1* (c.3969_3970insT) mutation was obtained by gene editing an established control iPSC line using CRISPR/Cas9 [34]. Two X-linked OI iPSC lines harboring the c.1376A>G (p.N459S) mutation in *MBTPS2* gene were reported by Tongkobpetch *et al*. [35]. An OI patient-specific iPSC line harboring the *COL1A1*, c.3162delT mutation was established by employing the Sendai virus [36]. Another OI-specific iPSC line was constructed by *in vitro* reprogramming of PBMCs from an OI type IV patient harboring a heterozygous c.928G>A (p.G328S) mutation in the *COL1A2* gene [37]. Howden *et al*. [38] generated an OI iPSC line carrying a heterozygous mutation (*COL1A1* c.3936G>T) from fibroblasts and an isogenic gene-rectified control iPSC line. Using osteoblasts differentiated from OI iPSCs as a research model, Takeyari *et al.* [39] demonstrated that 4-phenylbutyric acid (4-PBA) has the ability to promote the mineralization of derived OI osteoblasts with a glycine substitution mutation and has the potential to serve as a novel therapeutic agent for OI. Duangchan *et al.* [40] generated two OI iPSCs lines with glycine substitution mutations in COL1A1 and COL1A2 and studied the effects of 4-PBA on the osteogenesis of OI iPSC-derived MSCs. Moreover, extensive OI mechanism studies have been performed following osteogenesis differentiation of OI-iPSCs [41,42]. These encouraging results inspired us to construct OI-specific iPSCs harboring our reported novel *COL1A1* mutation, which could provide a predictive cellular modeling platform for OI pathological study and drug screening. In contrast to the methods employed for acquiring donor cells from other sources, the collection of PBMCs used in our study was safe and did not have extraneous contamination. We generated two iPSC lines from the OI family. OI-iPSCs from the proband's affected son carrying a point mutation (G242V) in exon 10 of the *COL1A1* gene and HC-iPSCs from the proband's unaffected daughter who did not carry the mutation. We studied the morphology and characterized the iPSC lines. Our results demonstrated that these two cell lines showed morphologic characteristics similar to those of hESCs, and expressed pluripotent markers. Both OI-iPSCs and HC-iPSCs could form teratomas that included cell of three germ layers *in vivo*. They possessed the normal chromosome karyotype and an STR profile that was identical to primary donor cells, indicating that iPSC population shared the same genetic makeup as their initial donor cells. This formation and characterization of human PBMC-derived OI-iPSCs and HC-iPSCs could provide an excellent human genetic system for future studies uncovering the pathophysiological basis of OI. In future studies, we plan to generate OI-iPSC-derived osteoblasts that recapitulates the pathogenesis of OI, which will be used to investigate disease mechanisms and for drug screening.

5. Conclusions

This study reported an OI family. The mutation in the proband and her two affected children was detected to be heterozygous in *COL1A*1 exon 10, c.725G>T (nucleotide: NM_000088.3, GRCh37) predicting a p.G242V substitution (protein: NP_000079.1). Two iPSC lines (one patient-specific iPSC line and one family healthy donor iPSC line) were generated and characterized. The detailed genotyping of the OI family and establishment of iPSCs from an OI patient and healthy family member will be useful for investigating the mechanisms of OI and developing drug novel therapies.

Availability of Data and Materials

The data and materials generated during the current study are available from the corresponding author.

Author Contributions

DL, conception and design, data collection, data analysis, manuscript writing, review and editing; MO, conception and design, data collection, financial support, review and editing; GD, data analysis, financial support, review and editing; PZ, conception and design, data collection, financial support, review and editing; QL, data analysis, review and editing; JC, data analysis, review and editing; ZS, data collection, review and editing; IMS, conception and design, review and editing; LY, supervision, conception and design, review and editing; GS, financial support, conception and design, review and editing; DT, conception and design, data collection, review and editing; YD, conception and design, data collection, supervision and financial support, review and editing. All authors contributed to editorial changes in the manuscript. All authors have reviewed it critically for important intellectual and approved final manuscript. All authors have participated sufficiently in the work to take public responsibility for appropriate portions of the content and agreed to be accountable for all aspects of the work in ensuring that questions related to its accuracy or integrity.

Ethics Approval and Consent to Participate

This study received approval from the Medical Ethics Committee of Shenzhen People's Hospital (Shenzhen, China), in accordance with the ethical guidelines outlined in the Declaration Helsinki for conducting medical research involving human subjects. All subjects included in this study gave written informed consent to participate. The permission was obtained from the participants to use their photographs. Animal studies were approved by Jinan University Laboratory Animal Ethics Committee (20210301-38).

Acknowledgment

We thank all participants for their participation in this study.

Funding

This work was supported by the Science and Technology Planning Project of Guangdong Province, China (2017B020209001), the National Natural Science Foundation of China (82060393), the Science and Technology Plan of Shenzhen (JCYJ20180305163846927), the Natural Science Foundation of Guangxi (2020GXNSFAA159124), the Natural Science Foundation of Guangdong Province, China (2022A1515010378), the Scientific Research Project of Health System in Pingshan District of Shenzhen (202139, 201801, 202066, 202068) and RSF grant (22-15-20063).

Conflict of Interest

The authors declare no conflict of interest.

Supplementary Material

Supplementary material associated with this article can be found, in the online version, at https://doi.org/10.31083/j.fbl2812336.

References

[1] Marini JC, Forlino A, Bächinger HP, Bishop NJ, Byers PH, Paepe AD, *et al*. Osteogenesis imperfecta. Nature Reviews. Disease Primers. 2017; 3: 17052.

[2] Ashournia H, Johansen FT, Folkestad L, Diederichsen ACP, Brixen K. Heart disease in patients with osteogenesis imperfecta - A systematic review. International Journal of Cardiology. 2015; 196: 149–157.

[3] Forlino A, Cabral WA, Barnes AM, Marini JC. New perspectives on osteogenesis imperfecta. Nature Reviews. Endocrinology. 2011; 7: 540–557.

[4] Seto T, Yamamoto T, Shimojima K, Shintaku H. A novel *COL1A1* mutation in a family with osteogenesis imperfecta associated with phenotypic variabilities. Human Genome Variation. 2017; 4: 17007.

[5] Van Dijk FS, Pals G, Van Rijn RR, Nikkels PGJ, Cobben JM. Classification of Osteogenesis Imperfecta revisited. European Journal of Medical Genetics. 2010; 53: 1–5.

[6] Li L, Mao B, Li S, Xiao J, Wang H, Zhang J, *et al*. Genotypic and phenotypic characterization of Chinese patients with osteogenesis imperfecta. Human Mutation. 2019; 40: 588–600.

[7] Árvai K, Horváth P, Balla B, Tobiás B, Kató K, Kirschner G, *et al*. Next-generation sequencing of common osteogenesis imperfecta-related genes in clinical practice. Scientific Reports. 2016; 6: 28417.

[8] Hendrickx G, Boudin E, Van Hul W. A look behind the scenes: the risk and pathogenesis of primary osteoporosis. Nature Reviews. Rheumatology. 2015; 11: 462–474.

[9] Antoniazzi F, Pietrobelli A, Gandini A, Cavarzere P, Ramaroli DA, Mottes M, *et al*. Type VI Osteogenesis imperfecta: effect of plasma transfusion on bone metabolism. Journal of Biological Regulators and Homeostatic Agents. 2021; 35: 41–51.

[10] Forlino A, Marini JC. Osteogenesis imperfecta. Lancet (London, England). 2016; 387: 1657–1671.

[11] Lim J, Grafe I, Alexander S, Lee B. Genetic causes and mechanisms of Osteogenesis Imperfecta. Bone. 2017; 102: 40–49.

[12] Kruger KM, Caudill A, Rodriguez Celin M, Nagamani SCS, Shapiro JR, Steiner RD, *et al*. Mobility in osteogenesis imperfecta: a multicenter North American study. Genetics in Medicine: Official Journal of the American College of Medical Genetics. 2019; 21: 2311–2318.

[13] Kang H, Shih YRV, Nakasaki M, Kabra H, Varghese S. Small molecule-driven direct conversion of human pluripotent stem cells into functional osteoblasts. Science Advances. 2016; 2: e1600691.
[14] Rowe RG, Daley GQ. Induced pluripotent stem cells in disease modelling and drug discovery. Nature Reviews. Genetics. 2019; 20: 377–388.
[15] Sharma TP, Wiley LA, Whitmore SS, Anfinson KR, Cranston CM, Oppedal DJ, *et al*. Patient-specific induced pluripotent stem cells to evaluate the pathophysiology of TRNT1-associated Retinitis pigmentosa. Stem Cell Research. 2017; 21: 58–70.
[16] Park IH, Arora N, Huo H, Maherali N, Ahfeldt T, Shimamura A, *et al*. Disease-specific induced pluripotent stem cells. Cell. 2008; 134: 877–886.
[17] Ebert AD, Svendsen CN. Human stem cells and drug screening: opportunities and challenges. Nature Reviews. Drug Discovery. 2010; 9: 367–372.
[18] Lee G, Studer L. Induced pluripotent stem cell technology for the study of human disease. Nature Methods. 2010; 7: 25–27.
[19] Lee KS, Song HR, Cho TJ, Kim HJ, Lee TM, Jin HS, *et al*. Mutational spectrum of type I collagen genes in Korean patients with osteogenesis imperfecta. Human Mutation. 2006; 27: 599.
[20] Yu J, Chau KF, Vodyanik MA, Jiang J, Jiang Y. Efficient feeder-free episomal reprogramming with small molecules. PLoS ONE. 2011; 6: e17557.
[21] Sillence DO, Senn A, Danks DM. Genetic heterogeneity in osteogenesis imperfecta. Journal of Medical Genetics. 1979; 16: 101–116.
[22] Dalgleish R. The human type I collagen mutation database. Nucleic Acids Research. 1997; 25: 181–187.
[23] Robey PG, Fedarko NS, Hefferan TE, Bianco P, Vetter UK, Grzesik W, *et al*. Structure and molecular regulation of bone matrix proteins. Journal of Bone and Mineral Research: the Official Journal of the American Society for Bone and Mineral Research. 1993; 8 Suppl 2: S483–S487.
[24] Naomi R, Ridzuan PM, Bahari H. Current Insights into Collagen Type I. Polymers. 2021; 13: 2642.
[25] Andriotis OG, Chang SW, Vanleene M, Howarth PH, Davies DE, Shefelbine SJ, *et al*. Structure-mechanics relationships of collagen fibrils in the osteogenesis imperfecta mouse model. Journal of the Royal Society, Interface. 2015; 12: 20150701.
[26] Adams SL. Collagen gene expression. American Journal of Respiratory Cell and Molecular Biology. 1989; 1: 161–168.
[27] Ghosh DK, Udupa P, Shrikondawar AN, Bhavani GS, Shah H, Ranjan A, *et al*. Mutant MESD links cellular stress to type I collagen aggregation in osteogenesis imperfecta type XX. Matrix Biology: Journal of the International Society for Matrix Biology. 2023; 115: 81–106.
[28] Doan ND, Hosseini AS, Bikovtseva AA, Huang MS, DiChiara AS, Papa LJ, 3rd, *et al*. Elucidation of proteostasis defects caused by osteogenesis imperfecta mutations in the collagen-α2(I) C-propeptide domain. The Journal of Biological Chemistry. 2020; 295: 9959–9973.
[29] Udupa P, Shrikondawar AN, Nayak SS, Shah H, Ranjan A, Girisha KM, *et al*. Deep intronic mutation in CRTAP results in unstable isoforms of the protein to induce type I collagen aggregation in a lethal type of osteogenesis imperfecta type VII. Biochimica et Biophysica Acta. Molecular Basis of Disease. 2023; 1869: 166741.
[30] Takahashi K, Yamanaka S. Induction of pluripotent stem cells from mouse embryonic and adult fibroblast cultures by defined factors. Cell. 2006; 126: 663–676.
[31] Sharma A, Sances S, Workman MJ, Svendsen CN. Multi-lineage Human iPSC-Derived Platforms for Disease Modeling and Drug Discovery. Cell Stem Cell. 2020; 26: 309–329.
[32] Kimbrel EA, Lanza R. Next-generation stem cells - ushering in a new era of cell-based therapies. Nature Reviews. Drug Discovery. 2020; 19: 463–479.
[33] Soldner F, Jaenisch R. Medicine. iPSC disease modeling. Science (New York, N.Y.). 2012; 338: 1155–1156.
[34] Hosseini Far H, Patria YN, Motazedian A, Elefanty AG, Stanley EG, Lamandé SR, *et al*. Generation of a heterozygous COL1A1 (c.3969_3970insT) osteogenesis imperfecta mutation human iPSC line, MCRIi001-A-1, using CRISPR/Cas9 editing. Stem Cell Research. 2019; 37: 101449.
[35] Tongkobpetch S, Rungsiwiwut R, Pruksananonda K, Suphapeetiporn K, Shotelersuk V. Generation of two human iPSC lines (MDCUi001-A and MDCUi001-B) from dermal fibroblasts of a Thai patient with X-linked osteogenesis imperfecta using integration-free Sendai virus. Stem Cell Research. 2019; 39: 101493.
[36] Kim BY, Ko JM, Park MH, Koo SK. Generation of a patient-specific induced pluripotent stem cell line, KSCBi006-A, for osteogenesis imperfecta type I with the COL1A1, c.3162delT mutation. Stem Cell Research. 2019; 41: 101622.
[37] Zheng Z, Lu W, Pei Z, Chen J, Yang T, Luo F. Generation of an induced pluripotent stem cell line (CHFUi001-A) from an osteogenesis imperfecta patient with COL1A2 mutation. Stem Cell Research. 2020; 47: 101907.
[38] Howden S, Hosseini Far H, Motazedian A, Elefanty AG, Stanley EG, Lamandé SR, *et al*. The use of simultaneous reprogramming and gene correction to generate an osteogenesis imperfecta patient COL1A1 c. 3936 G>T iPSC line and an isogenic control iPSC line. Stem Cell Research. 2019; 38: 101453.
[39] Takeyari S, Kubota T, Ohata Y, Fujiwara M, Kitaoka T, Taga Y, *et al*. 4-Phenylbutyric acid enhances the mineralization of osteogenesis imperfecta iPSC-derived osteoblasts. The Journal of Biological Chemistry. 2021; 296: 100027.
[40] Duangchan T, Tawonsawatruk T, Angsanuntsukh C, Trachoo O, Hongeng S, Kitiyanant N, *et al*. Amelioration of osteogenesis in iPSC-derived mesenchymal stem cells from osteogenesis imperfecta patients by endoplasmic reticulum stress inhibitor. Life Sciences. 2021; 278: 119628.
[41] Deyle DR, Khan IF, Ren G, Wang PR, Kho J, Schwarze U, *et al*. Normal collagen and bone production by gene-targeted human osteogenesis imperfecta iPSCs. Molecular Therapy: the Journal of the American Society of Gene Therapy. 2012; 20: 204–213.
[42] Kawai S, Yoshitomi H, Sunaga J, Alev C, Nagata S, Nishio M, *et al*. In vitro bone-like nodules generated from patient-derived iPSCs recapitulate pathological bone phenotypes. Nature Biomedical Engineering. 2019; 3: 558–570.